THE AMERICAN MINERALOGIST, VOL. 55, MAY-JUNE, 1970

INTERFERENCE COLORS IN FLASH FIGURES

BARCLAY KAMB, *Division of Geological Sciences*,[1] *California Institute of Technology, Pasadena, California 91109.*

ABSTRACT

The distribution of colors in interference figures of crystal plates of arbitrarily large thickness and birefringence cannot be treated with the conventional path-difference formula that is the basis for the use of Bertin's surfaces, but the correct path-difference formula is nevertheless simple. When applied to the uniaxial flash figure, it shows that the color will always fall continuously from the center of the figure toward the optic axes, contrary to statements in some textbooks. For most biaxial flash figures, the color will decrease toward the acute bisectrix and increase toward the obtuse bisectrix. However, for a limited range of figures near $2V=90°$, the color can at first decrease and then begin to increase subsequently toward the acute bisectrix, an effect similar to that envisaged in the textbook statements mentioned.

INTRODUCTION

The distribution of interference colors in flash figures is in principle a point of importance in understanding the effects of crystal optics that are shown in interference figures. In practice, the distribution of colors is not ordinarily used to ascertain the position of the optic plane, but occasionally it may be helpful, as when the isogyres are too diffuse for their motion to be observed clearly. The color effect normally seen in a flash figure is a fall in interference color from the center of the figure (optic normal) toward the periphery in the direction of the acute bisectrix (or optic axis of a uniaxial crystal), and a rise in color in the direction perpendicular thereto. However, a statement has occasionally appeared in textbooks (Johanssen, 1914, p. 420; Bloss, 1961, p. 122; Wahlstrom, 1951, p. 216 [but not in later editions]) to the effect that in flash figures obtained from uniaxial crystal plates of high birefringence or large thickness, the interference color at first falls in the direction toward the optic axis, but farther out from the center the color begins to rise. I will show that this statement is incorrect as applied to the uniaxial flash figure, but that in certain biaxial flash figures an effect of the type described can in principle occur.

PRINCIPLES GOVERNING PATH DIFFERENCE IN CONOSCOPE

For a birefringent crystal plate of thickness t, the interference color to be seen at each point in the conoscopic field is determined from the relationships shown in Figure 1. An incoming polarized light wave CA from the condenser, travelling at an angle θ with respect to the microscope axis AM (which is normal to the crystal plate as shown), is resolved

[1] Contribution No. 1693.

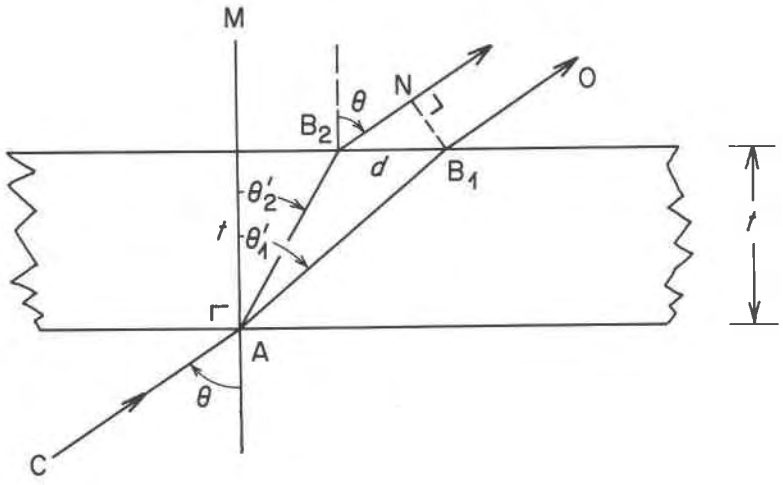

FIG. 1. Double refraction of light in a crystal plate of thickness t. An incident ray CA after double refraction propagates as separate rays with wave-normal directions AB_1 and AB_2, which after emergence from the plate again propagate along parallel paths B_1O and B_2N. MA is the direction of the microscope axis, normal to the crystal plate.

at A into two waves of different refractive index n_1' and n_2', which propagate through the crystal plate along the wave-normal directions AB_1 and AB_2, which lie in the plane of incidence defined by CA and AM (plane of the drawing). The refracted inclinations of these wave normals, θ_1' and θ_2', are not equal if the crystal plate is birefringent. They satisfy Snell's law, in terms of the wave indices n_1' and n_2':

$$\begin{aligned} n_1' \sin \theta_1' &= \sin \theta \\ n_2' \sin \theta_2' &= \sin \theta \end{aligned} \tag{1}$$

In writing (1), the refractive index of air is taken to be 1. Equations (1) remain valid if plane-parallel sheets of other isotropic media (glass, Canada balsam) bound the crystal plate on either or both sides, the angle θ being the inclination, *in air*, of the incident ray CA and also the emerging rays B_1O and B_2N.

The emerging rays B_1O and B_2N are combined in the conoscope, coming to a common focus in the interference surface of the objective lens. Beyond the points B_1 and N_1 their phase difference remains unchanged; hence the phase difference or path difference that is seen as an interference color in the conoscope field is that accumulated over the paths AB_2N and AB_1. Here B_1N represents a wave front and is therefore perpendicular to B_2N. The optical path difference Δs can be computed from Figure 1 in the standard way (physical path length times refractive

index equals optical path length):

$$\Delta s = n_2' \frac{t}{\cos \theta_2'} + d \sin \theta - n_1' \frac{t}{\cos \theta_1'} \tag{2}$$

In drawing Figure 1 and in writing down equation (2), we assume that $n_2' > n_1'$, but the final result, equation (4) below, turns out to be independent of this assumption. d in (2) is the distance between B_1 and B_2, which is

$$d = t(\tan \theta_1' - \tan \theta_2') \tag{3}$$

Combining (1), (2), and (3) gives

$$\Delta s = t(n_2' \cos \theta_2' - n_1' \cos \theta_1') \tag{4}$$

Equation (4), in combination with (1), gives the path difference at a point in the conoscope field defined by the ray inclination θ in air outside the crystal plate. It is valid for arbitrarily large birefringence $\Delta n' \equiv n_2' - n_1'$ and plate thickness t.

If the birefringence is small, it is useful to expand (4) in powers of $\Delta n'$, and obtain

$$\Delta s = \frac{t \Delta n'}{\cos \theta_1'} - \frac{t(\Delta n')^2}{2n} \tan^2 \theta_1' \sec \theta_1' + \cdots \tag{5}$$

the omitted terms being of still higher order in $\Delta n'$. If the second order term is neglected, (5) becomes, approximately,

$$\Delta s \cong \frac{t \Delta n'}{\cos \theta'} \tag{6}$$

where θ' can represent either θ_1' or θ_2' in the approximation of small $\Delta n'$. Equation (6) is the expression for path difference commonly given in texts (e.g. Wahlstrom, 1969, p. 242, eqn. (10–1)). It neglects the difference between the propagation directions θ_1' and θ_2' of the refracted waves in the crystal plate. By the derivation of (6) from (4), it is evident that this neglect becomes valid in the approximation of small birefringence ($|\Delta n'| << 1$). Equation (6) is the basis for the use of Bertin's surfaces in interpreting the color patterns in interference figures.

It is worthwhile to point out a great difference between the predicted behavior of the path difference Δs at large inclination angles θ', as given on the one hand by (4) and on the other by (6). According to (6), at large θ' ($\rightarrow 90°$) the value of Δs increases without bound (unless $\Delta n' \rightarrow 0$ fast enough as $\theta' \rightarrow 90°$), whereas according to (4) the value of Δs remains finite for any refracted angles θ_1' and θ_2'. It is clear from (5) that as

$\theta_1' \to 90°$, the second order term (and probably the higher order terms also) cannot be neglected no matter how small the value of $\Delta n'$ (assuming $\Delta n' \neq 0$). Thus the approximate validity of the common formula (6) is restricted not only to small $\Delta n'$ but also to sufficiently small θ'. The underlying reason for the finiteness of the path difference given by (4) as θ_1' and θ_2' become large is perhaps not obvious intuitively, since for large θ_1' and θ_2' the physical path lengths become very large (they increase without bound as θ_1' and θ_2' approach 90°). The finite optical path difference is traceable to the fact that for large inclinations, a small difference between θ_1' and θ_2' results in a large difference in the proportions of the physical paths that are traversed inside and outside the crystal plate for the two separate refracted waves.

Flash Figures

The distribution of interference colors in the flash figure of a crystal plate of arbitrary birefringence and thickness is a matter of applying (1) and (4) to a special case. We suppose that the optic normal stands vertical, parallel to AM in Figure 1, and for simplicity we investigate the color distribution only in the principal planes of the indicatrix, that is, along radial lines in the interference figure from the center outward toward the *Bxa* and toward the *Bxo*. Figure 2 shows the appropriate principal section of the indicatrix. We choose the vibration direction for n_1' to be the one along the principal axis normal to the plane of incidence (plane of drawing in Fig. 2). For definiteness we take this indicatrix axis to be n_1. The principal indices will be ordered either $n_1 \leqq n_2 \leqq n_3$ or $n_1 \geqq n_2 \geqq n_3$, n_2 always being the intermediate principal index. n_1' is independent of θ_1', but n_2' depends on θ_2' as shown by the elliptical section of the indicatrix in Fig. 2:

$$n_1' = n_1$$
$$\frac{(n_2' \cos\theta_2')^2}{n_3^2} + \frac{(n_2' \sin\theta_2')^2}{n_2^2} = 1 \tag{7}$$

Equations (1), (4), and (7) can be combined to give the desired path difference along a radial line toward the bisectrix:

$$\frac{\Delta s'}{t} = n_3 \sqrt{1 - \frac{\sin^2\theta}{n_2}} - \sqrt{n_1 - \sin^2\theta} \tag{8}$$

Uniaxial Flash Figure

If we set $n_1 = n_2 = \omega$, and $n_3 = \epsilon$, then equation (8) describes the special case of a uniaxial flash figure traversed along a radial line toward the

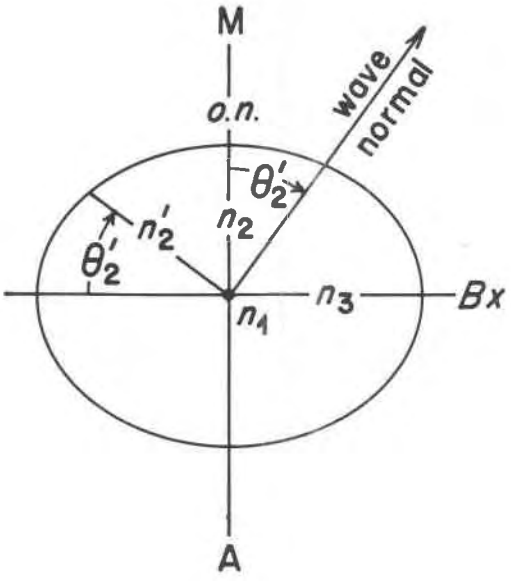

FIG. 2. Principal section of the indicatrix to correspond with Fig. 1 for the case of a flash figure traversed along a radial line toward the bisectrix Bx. The optic normal is $o.n.$ and the bisectrix Bx is taken to correspond to principal refractive index n_3.

optic axis:

$$\frac{\Delta'}{t} = (\epsilon - \omega)\sqrt{1 - \frac{\sin^2\theta}{\omega^2}} \tag{9}$$

From the form of (9) it is clear that the path difference always decreases continuously from the center of the figure ($\theta=0$) toward the periphery, no matter how large a conoscopic angle θ (less than 90°, of course) is visible. This conclusion is valid, as is (9), for arbitrarily large birefringence $\epsilon-\omega$ and arbitrarily large thickness t. It contradicts the textbook statements noted earlier.

For completeness we may derive also from (8) the color distribution along the radial line perpendicular to the optic axis. For this purpose, set $n_2=n_3=\omega$, $n_1=\epsilon$, and obtain

$$\begin{aligned}\frac{\Delta s'}{t} &= \sqrt{\omega^2 - \sin^2\theta} - \sqrt{\epsilon^2 - \sin^2\theta} \\ &= \frac{\omega^2 - \epsilon^2}{\sqrt{\omega^2 - \sin^2\theta} + \sqrt{\epsilon^2 - \sin^2\theta}}\end{aligned} \tag{10}$$

Because both terms in the denominator of (10) decrease with increasing θ, it is clear that the interference color in this case increases progressively outward to arbitrarily large conoscopic angles.

Biaxial Flash Figure

To describe the color distribution in a biaxial flash figure, we return to (8). From the form of (8) as its stands, it is difficult to tell what radial color variation is predicted, but an expansion in powers of $\sin\theta$ is helpful:

$$\frac{\Delta s}{t} = (n_3 - n_1) + \frac{1}{2}\,\frac{n_2^2 - n_1 n_3}{n_2^2 n_1}\sin^2\theta + \frac{1}{8}\,\frac{n_2^4 - n_3 n_1^3}{n_2^4 n_1^3}\sin^4\theta + \cdots \tag{11}$$

To a first approximation, the radial color variation near the center of the interference figure is described by the $\sin^2\theta$ term on the right side of (11). If the intermediate principal index n_2 is the geometric mean of the largest and smallest principal indices, *i.e.* $n_2 = \sqrt{n_1 n_3}$, then to the first approximation there is no radial color variation. The geometric mean condition for n_2 is not precisely the condition for $2V = 90°$, but it is close, and the two conditions become the same as the birefringence tends to zero. If n_2 is closer to n_1 than would be true for the geometric mean condition, then the first and second terms on the right side of (11) have opposite sign, and the interference color falls radially. This is essentially the case when axis 3 is the acute bisectrix, so that we may expect the colors to fall toward the acute bisectrix. Similarly, a rise toward the obtuse bisectrix is expected, for in this case (n_2 closer to n_3 than would be true for the geometric mean condition), the first and second terms on the right in (11) have the same sign. These conclusions are most easily verified in the case of small birefringence. If we express the indices as

$$\begin{aligned} n_3 &= n_2 + \epsilon_3 \\ n_1 &= n_2 - \epsilon_1 \end{aligned} \tag{12}$$

and suppose ϵ_3 and ϵ_1 to be small quantities, then to lowest order in ϵ_1 and ϵ_3, (11) becomes

$$\frac{\Delta s}{t} \cong (n_3 - n_1) + \frac{1}{2}\,\frac{\epsilon_1 - \epsilon_3}{n_2^2}\sin^2\theta + \frac{1}{8}\,\frac{3\epsilon_1 - \epsilon_3}{n_2^4}\sin^4\theta + \cdots \tag{13}$$

In the approximation of small birefringence, $\epsilon_1 = \epsilon_3$ is equivalent to $2V = 90°$.

The radial fall in color toward the acute bisectrix can reverse toward the periphery of the conoscopic field if the $\sin^4\theta$ term in (11) has opposite sign from the $\sin^2\theta$ term. The angle θ at which the reversal occurs will be that for which $d\Delta s/d\theta = 0$, and the condition for this can be found without any approximations by differentiating (8), giving:

$$\frac{d\Delta s}{d\theta} = 0 \quad \text{at } \theta = \theta_R,$$

where

$$\sin^2\theta_R = \frac{n_3^2 n_1^2 - n_2^4}{n_3^2 - n_2^2} \tag{14}$$

The range of conditions over which a reversal effect can theoretically occur corresponds to a variation in θ_R in (14) from $\theta_R = 0$ to $\theta_R \approx 90°$, approximately the practical conoscopic limit even for oil-immersion conoscopes. [Theoretically, for an oil-immersion system the quantity sin θ (where θ is defined as the conoscopic angle *in air*) can actually increase to the N.A. of the objective, which is as large as 1.25 for standard oil-immersion objectives.] In the case of small birefringence, (12), for which (14) becomes

$$\sin^2\theta_R \cong n_2^2 \frac{\epsilon_3 - \epsilon_1}{\epsilon_3}, \tag{15}$$

the range $\theta_R = 0°$ to 90° corresponds to a range in $2V$ (about axis 3) from 90° to 76°, as calculated for $n_2 = 1.60$.

A more stringent limit on observability of the reversal effect is obtained by requiring that Δs at $\theta = 90°$ be the same as at $\theta = 0°$. In this case, a reversal must take place within the θ range 0° to 90°, since near the center there is an initial radial fall in color as shown by (13). The above requirement corresponds, from (8), to the following condition on the refractive indices:

$$\frac{n_3}{n_2} = \frac{\sqrt{n_2^2 - 1} + n_2}{\sqrt{n_1^2 - 1} + n_1} \tag{16}$$

For small birefringence, (16) becomes

$$\frac{\epsilon_1}{\epsilon_3} = \frac{\sqrt{n^2 - 1}}{n_2} \tag{17}$$

and for $n_2 = 1.60$, the corresponding lower limit on $2V$, for the reversal effect to occur along the radius toward the acute bisectrix, is $2V = 83°$.

The reversal effect does not depend in principle on thickness of the crystal plate, contrary to the textbook statements mentioned earlier. On the other hand, the amplitude of the initial decrease and subsequent increase in path difference indicated by (8) or (11) will be increased in proportion to plate thickness, and the effect is therefore more likely to be detectable for plates of large thickness.

Increased birefringence also tends to increase the amplitude of the effect, but as the birefringence becomes finite, a complication enters. The limiting condition $n_2 = \sqrt{n_1 n_3}$ that is pertinent in (11) and (14) corresponds to

$$\tan^2 V_3 = \frac{n_3}{n_1} \tag{18}$$

where V_3 is measured about axis 3. At this limiting condition, (11) becomes

$$\frac{\Delta s}{t} = (n_3 - n_1) + \frac{1}{8} \frac{n_3 - n_1}{n_2^2 n_1^2} \sin^4 \theta + \cdots \tag{19}$$

which shows that at the limiting condition, the radial color variation near $\theta = 0$ will be an outward increase both toward the *Bxa* and the *Bxo*. If $n_3 > n_1$, then actually axis 1 is the *Bxa*; for example, if $n_1 = 1.50$ and $n_3 = 1.80$, then $2V_1$, about axis 1, is 84.8° at the limiting condition $n_2 = \sqrt{n_1 n_3}$. As we depart from this limiting condition in the direction that makes the optic axes close together about axis 1, that is $n_2 > \sqrt{n_1 n_3}$ in case $n_3 > n_1$, then the reversal effect will appear in the quadrant of the conoscopic field containing axis 1, and, conversely, for n_2 slightly less than $\sqrt{n_1 n_3}$, the reversal effect will move into the quadrant containing axis 3, even though this axis is not yet the *Bxa*. From this situation we can infer that for biaxial negative crystals of large birefringence, the reversal effect can be observed at somewhat lower $2V$ than for biaxial positive crystals. As an actual example, we may choose $n_2 = 1.70$, $n_3 = 1.90$, and from (14) calculate $n_1 = 1.558$ for $\theta_R = 90°$. This is the biaxial positive case. For the biaxial negative case, we can interchange the roles of n_3 and n_1 in (14), and again calculate n_1 for $\theta_R = 90°$, giving $n_1 = 1.446$. For the reversal effect to occur, the lowest biaxial positive $2V$ is thus $2V_Z = 82.2°$, whereas the lowest biaxial negative $2V$ is $2V_X = 77.5°$. In the results for this example there is no indication that high birefringence increases the total range of $2V$ over which the reversal effect could theo-

retically be observed. In fact, the total range is much more dependent on n_2 than on the birefringence, as shown by (15), from which we can infer that effect is more likely to be observed for crystals of low mean refractive index. This is due simply to the fact that the effective conoscopic field (maximum θ_1' and θ_2') is increased for low mean refractive index.

Acknowledgment

I was prompted to publish the above results by the receipt of a manuscript by Robert Greenwood, which discussed the uniaxial flash figure on the basis of equation (6) above. I wish to thank Dr. Greenwood for the stimulus thus provided. A treatment of the uniaxial flash figure on the basis of (6) leads qualitatively to the same conclusions as those based on (4), because as the optic axis is approached, Δn tends to zero rapidly enough to offset the effect of the cos θ' factor. For the biaxial flash figure this does not happen, so that a qualitative as well as quantitative discrepancy between the results of (4) and (6) would arise in this case.

References

Bloss, F. D. (1961) *An Introduction to the Methods of Optical Crystallography*. Holt, Rinehart, & Winston, New York, 294 p.

Johanssen, A. (1941) *Manual of Petrographic Methods*. McGraw-Hill, New York, 649 p.

Wahlstrom, E. E. (1951) *Optical Crystallography*, 2nd ed. Wiley & Sons, New York, 247 p.

——— (1969) *Optical Crystallography*, 4th ed. Wiley & Sons, New York, 489 p.

Manuscript received, November 17, 1969; accepted for publication, January 3, 1970.

Note Added in Proof

I find that the basic path-difference formula, Equation (4), has been given previously by C. Burri [*Das Polarisationsmikroscope*. Birkhaüser, Basel, Equation (A43), p. 63, (1950)], and in fact was derived originally by F. Neumann in 1834. The present derivation (which was made without knowledge of the earlier work) may help, I hope, to introduce this basic formula into the English-language literature of crystal optics. The formula has been used by R. Rath [Exakte Darstellung der isochromatischen Kurven, *Neues Jarb. Mineral. Abh.* **108,** 131, (1968)], for calculating the shapes of isochromatic curves in interference figures, but it has not previously been applied to the problem of the present paper, as far as I know.